catalysts

MDPI

Review

Bimetallic Catalysts Containing Gold and Palladium for Environmentally Important Reactions

Ahmad Alshammari [1,*], V. Narayana Kalevaru [2] and Andreas Martin [2,*]

[1] Materials Science Research Institute (MSRI), King Abdulaziz City for Science and Technology (KACST), P. O. Box 6086, Riyadh 11442, Saudi Arabia

[2] Department of Heterogeneous Catalytic Processes, Leibniz Institute for Catalysis, Albert-Einstein-Str. 29a, Rostock 18059, Germany; narayana.kalevaru@catalysis.de

* Correspondence: aalshammari@kacst.edu.sa (A.A.); andreas.martin@catalysis.de (A.M.); Tel.: +966-11-481-4285 (A.A.); +49-381-1281-246 (A.M.)

Academic Editor: John R. (JR) Regalbuto
Received: 11 April 2016; Accepted: 24 June 2016; Published: 5 July 2016

Abstract: Supported bimetallic nanoparticles (SBN) are extensively used as efficient redox catalysts. This kind of catalysis particularly using SBN has attracted immense research interest compared to their parent metals due to their unique physico-chemical properties. The primary objective of this contribution is to provide comprehensive overview about SBN and their application as promising catalysts. The present review contains four sections in total. Section 1 starts with a general introduction, recent progress, and brief summary of the application of SBN as promising catalysts for different applications. Section 2 reviews the preparation and characterization methods of SBN for a wide range of catalytic reactions. Section 3 concentrates on our own results related to the application of SBN in heterogeneous catalysis. In this section, the oxidation of cyclohexane to adipic acid (an eco-friendly and novel approach) will be discussed. In addition, the application of bimetallic Pd catalysts for vapor phase toluene acetoxylation in a fixed bed reactor will also be highlighted. Acetoxylation of toluene to benzyl acetate is another green route to synthesize benzyl acetate in one step. Finally, Section 1 describes the summary of the main points and also presents an outlook on the application of SBN as promising catalysts for the production of valuable products.

Keywords: bimetallic catalysts; Pd-Sb catalysts; Au-Ag catalysts; acetoxylation; oxidation

1. Introduction

1.1. General Introduction

In this technological age of continuously growing demands, a lot of stringent restrictions are being imposed on the chemical industry to safeguard the environment and also to develop novel, economically attractive, clean and green processes. Recent advances made in catalyst technology are attempting to meet these challenges by means of applying a wide range of possibilities, e.g., employing more sustainable feedstocks, application of more efficient catalysts having two or more components (e.g., metals/metal oxides) to generate bifunctional and multi-functional properties etc. Bimetallic catalysts, in particular, are an important class of heterogeneous catalysts due to their unusual catalytic properties compared to their individual metal components [1–3]. In other words, metal particles composed of two different metal components exhibit different catalytic properties to monometallic catalysts. Such bimetallic catalysts not only reveal the combination of the properties related to the presence of two individual metals, but also generate new and distinctive properties due to synergetic effects between the two metals present. The structure of the bimetallic particles can be oriented in random, for instance alloy or intermetallic compound, cluster-in-cluster or core-shell structures etc.

However, their final structure strongly depends upon the composition, their synthesis method and conditions, relative strengths of metal-metal bond, surface energies of bulk elements etc. A study on bimetallic catalyst activity was initiated by the Exxon Research and Engineering Company in 1960 and John H. Sinfelt coined the term bimetallic cluster for a dispersed supported metallic catalyst of silica and alumina in 1980 [3]. Many research activities have been focused in the last few decades on the relationship between metal electronic configuration and the actions of catalysts, which has ultimately resulted in the bimetallic catalyst becoming one of the most prominent categories of heterogeneous catalysts [4]. The first research was carried out on bimetallic catalysts using Ni-Cr, Ru-Cu, Os-Cu, Pt-Ir, and Pt-Ru etc. The potential of these catalysts are evaluated for reactions such as hydrogenation, dehydrogenation, and isomerization process, which show that the valence electronic configuration of the metallic catalyst plays a key role on the activity and selectivity properties. In last few decades, the library of bimetallic catalyst has also been expanded very significantly. Many variations from GROUP VIII and GROUP IB have been investigated over the last thirty or more years and as a result there exists a significant wealth of research literature on bimetallic catalysts [5]. This field is now a rapidly expanding area within the manufacturing and chemistry process industry for different energy conversions [6].

The oxygen reduction in fuel cell technology is one of the many applications for bimetallic catalysts in a range of chemical reactions [7]. The effect of bimetallic catalysts on the development of biofuel from biomass was investigated by Alonso et al. and their findings indicated that bimetallic catalysts offer high activity, modified selectivity and improved stability for biomass conversion [8,9]. The range of applications of bimetallic catalysts in the chemical industry was a detailed studied by the group of Hutchings [10]. It was discovered by Wei et al. that in the production of H_2, selectivity towards H_2 can be monitored by using various blends of bimetallic catalysts [11]. Both the selectivity of reaction and the product output are controlled by the varying ratios of both metals in the catalyst of Ru-Cu for the catalysis of the hydrogenolysis of glycerol [12]. For hydrogenations, the bimetallic catalysts of Ru-Sn are used to vary the selectivity from hydrogenation of C=C to C=O whereas monometallic catalysts of Pt or Pd are more favorable in the hydrogenation of C=C bonds [13–15]. Moreover, several other important oxidation reactions were also carried out by various research groups using different compositions of bimetallic catalysts. For instance, Pd-Cu/TiO_2 catalysts were applied for selective oxidation of methanol to methyl formate and claimed 50% conversion of methanol with over 80% selectivity to methyl formate [16]. Recently, Sobczak et al. [17] used Au-Ag bimetallic catalysts supported on MCF (Mesostructured Cellular Foams) for the oxidation of methanol to formaldehyde. They report the formation of Au-Ag alloy on MCF surface that is responsible for high activity of the catalysts. In addition, bimetallic Au-Pd supported on 5A zeolite was applied for the synthesis of vinyl acetate from ethylene by vapor phase acetoxylation [18]. Moreover, some review articles also appear in the recent literature on the usage of noble metal based bimetallic catalysts for different catalytic applications. The investigations made by Zaleska-Medynska et al. [19] revealed that the nanoparticles composed of two different metal elements show novel electronic, optical, and catalytic properties that are different from monometallic nanoparticles. Their studies suggest that the bimetallic nanoparticles exhibit not only the combination of the properties related to the presence of two individual metals, but also generate new properties due to a synergy between two metals present.

Practically bimetallic catalysts are more advantageous than monometallic catalysts due to variations in their electronic configuration, the surface composition, the oxidation state etc. [20–22]. The properties of bimetallic nanoparticles were reviewed by Mohl et al. [23] and Huang et al. [24]. These authors claimed that both physico-chemical properties of nanoparticles were affected by both metals, i.e., the inclusion of a second metal creates a different set of properties [25]. Plasmonic coupling for different sensing applications is improved through the use of various combinations of metals [26]. Surface resonance causes very uniform optical properties in monometallic particles even though they become unique and tunable when the composition is varied, which can also reveal a significant effect on the local electric field [27,28]. The size, morphology, and composition of metallic nanoparticles are also

affected by the absorption, dispersion, and reflection of light [29]. If we look at the nanoparticles of gold and silver, it can be seen that they strongly absorb and scatter the light when they are smaller compared to the wavelength of visible light. Again, even if the composition is similar, the optical properties are changed by the variations in the structure of bimetallic nanoparticles [30]. According to the study of Ramakritinan et al. [31], Gram-positive and Gram-negative bacteria can be affected negatively by the bimetallic nanoparticles of silver and gold and also in the case of bimetallic nanoparticles (silver and gold) with a ratio of 1:3, the pathogenic bacteria are also prevented from growing. In this contribution, we describe the application of different Au and Pd based bimetallic catalysts for various industrially important and environmental friendly reactions.

1.2. Structures of Bimetallic Nanocatalysts

As shown in Figure 1, there are normally six different structures available for bimetallic catalysts: crown-jewel structure, hollow structure, hetero-structure, core-shell structure, and alloyed structure [32]. The Crown-jewel structure is described as being the case where the atoms of one of the elements are pulled together in a controlled fashion on the surface of the other metal at unique points. Expensive metals and atoms of expensive metals, jeweled at the crown of inexpensive metals, are the main use of this Crown-jewel structure. The two significant advantages of this type of catalysts are the efficient and effective use of precious metals with an aim of improving catalytic activity. The chemical vapor deposition method is the one most used method to make a crown-jewel structure whilst it has to be carefully managed at the atomic level. However, it is still a difficult piece of work and indeed the preparation of the Pd-Cu bimetallic catalyst by Sykes et al. used this methodology [33]. The Crown-jewel structure can also be produced using the solution state method but this is more difficult than the CVD approach, used by Toshima et al. for the production of Au-Pd nanocatalysts [34].

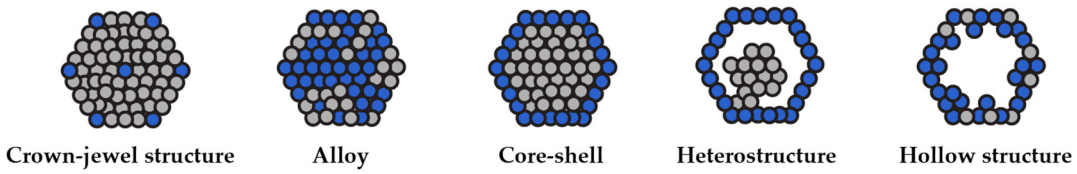

Figure 1. Schematic illustration of bimetallic nanoparticles with different structures.

The second method is the Hollow structure, which is becoming more popular due to its high surface to volume ratio. It also includes room for reactions with the active components being surrounded by an interior hollow structure [35,36]. In addition, the nanocatalysts have disparate catalytic properties from solid catalysts and with a lower density and hence the costs are reduced because of the fact that less amounts of materials are needed. The process for producing hollow structure nanoparticles is termed the template-mediated approach, which has three components namely hard templating, soft templating, and sacrificial templating [37].

The creation of hetero-structured particles through the wet-chemical preparation method of bimetallic nanocrystals causes two type of metals to nucleate and then grow on their own (heterogeneous seeded growth), because of varying standard reduction potentials. The situation where the seeds of one metal are used first as the sites for nucleation and then for the growth of another metal, is termed seed-mediated growth and is well known for creating bimetallic nanocrystals. Whichever of either layered, island or mixed growth type shown by the second metal determine the final morphology of the bimetallic structure. The factors that determine the nature of growth are as follows: lattice-matching structure, lattice-mismatching structure, surface and interface energy correlations, and the difference between the electronegativities of the two metals. For instance, improved catalytic activity in the proton exchange membrane can be achieved by using Pt-based hetero-nanocatalysts in the fuel cell [38]. Xia et al. claimed that the hetero-structure of Pd-Pt is almost

more active by factor of 2.5 compared to an equivalent mass of Pt created by using heterogeneous seeded growth [39].

The best high catalytic efficiency structure is known as the Core-shell structure, which is made from active metal shell, including a metal support [40]. The interior atoms are usually discarded or unused as most of the chemical reaction occurs on the surface of catalysts, with cheap metal being used to fabricate the interior side of the core-shell structure using a one-pot co-reduction or seed-mediated approach [41].

The last method is an alloyed structure where both of the metals are in homogeneous distribution and they are normally produced using a wet chemical synthesis method under carefully monitored reaction kinetics. Due to such careful integration of two metals alloyed bimetallic NPs are created [42]. The co-reduction method of two different types of metal ions is the popular way to create alloyed structured bimetallic NPs and this is facilitated by the use of a strong reducing agent. Noble metals such Ag, Au, Ru, Rh, Pd, or non-noble 3d transition metals like Cu, Co, Fe alloying with Pt is effective for forming electrocatalysts. An example of this approach was reported by Xu et al. where co-reduction was used to synthesize Ni-Fe alloyed structure nanoparticles [43]. Researchers were also able to create recently new structures with high surface area because that has become a crucial factor in chemical catalytic reactions [44].

1.3. Factors Affecting the Catalytic Activity of a Bimetallic Catalyst

Particle size and shape, structure, composition, surface area and porosity etc. are found to be the main factors that affect the catalytic properties of bimetallic catalysts in different reactions. Figure 2 represents the summary of these factors on the catalytic properties. Additionally, the effects of some other selected factors are also discussed in the following section.

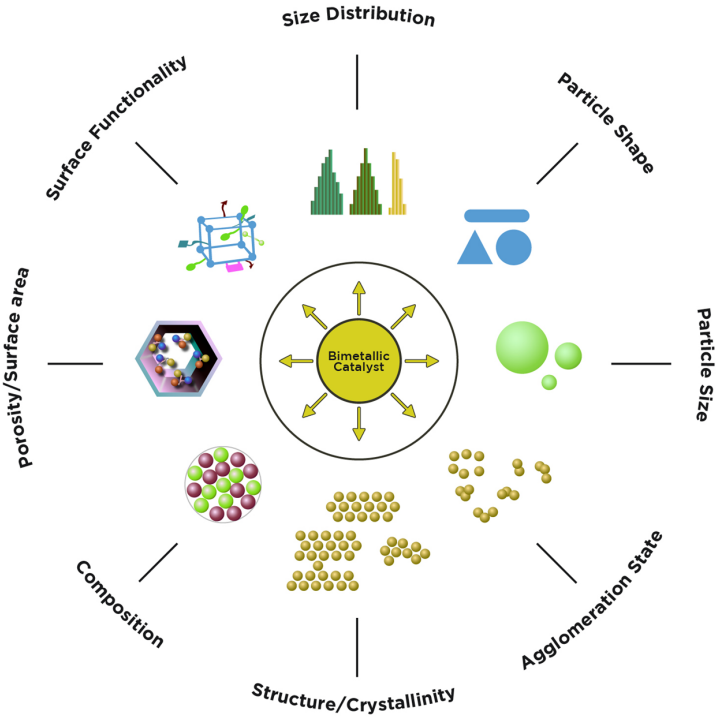

Figure 2. Factors affecting the catalytic properties of bimetallic catalysts in different reactions.

1.3.1. Effect of Particle Size and Shape

An increase in the catalytical performance using bimetallic catalysts can be obtained by tuning the size of the metal particles. The effect of particle size on the catalytic activity and selectivity of

supported metal nanoparticles was investigated extensively by Haruta et al. [45] The surface area will normally increase with decreasing size of metal particles as the total surface area of metal particles is contrariwise proportional to the square of the diameter of nanoparticles. Since the majority of the chemical reactions occur on the surface of the catalyst, hence with decreasing size of particles there is an increase in catalytic activity [46,47]. Slower reactions are caused by continuously decreasing the size of the nano-catalysts whereas increasing the size of the catalyst will decrease the rate of reaction. There is a critical size of metal particle (usually 3 nm) in photochemical hydrogen generation using nanocatalysts of Pt and any movement above or below will slow down the chemical reaction [48]. Lopez et al. discovered that particle size is a determining factor of catalyst performance as it is known to affect the selectivity of catalyst [49].

1.3.2. Structure Effect

Compared to mono-metallic catalyst systems, bimetallic catalysts with particular characteristics have improved adaptability in design for activity and selectivity of the catalyst. It is widely believed that the catalytic performance of mono- and bimetallic catalysts is strongly dependent on the particle size of the metals. The type of the support, the metal-support interface and structure effect are some of the other factors, which may also play a crucial role on the catalytic activity of bimetallic catalysts in various chemical reactions. Inter-metallic compounds, cluster-in-cluster or core-shell structures are the result of having two metals forming different destitution modes. It is important to realize that the preparation method of bimetallic catalysts is linked to the type of bimetallic structure. An efficient electrocatalytic activity of the oxidation of formic acid was observed using palladium nanoparticles. It is noted that using another type of metal nanoparticles such as gold has the effect of improving the catalytic performance and providing resistance to poisoning, however incorporating these metals leads to a significant change in their catalytic properties thus affecting their atomic distributions and improving their catalytic performance compared to the monometallic system. For instance, gold alone cannot oxidize formic acid directly but it improves the capability of CO oxidation by lowering the CO adsorption energy. To facilitate the oxidation step of formic acid there needs to be more available Pd active sites. Moreover, in the scenario where there are platinum-based nano-catalysts, Pt has the more active electronic configuration for oxygen reduction in the fuel cell. The selectivity of catalysts can be increased by reducing the fraction of Pt using another metal thus altering the electronic state of Pt affecting the distance between Pt-Pt bonds and the coordination number [50].

1.3.3. Composition Effects

Clear material composition with tunable interparticle distance is needed for the stability of catalysts in a chemical reaction. Roldan reported that the particle size is very crucial, as is that of the distribution on the substrate so that the lifetime of the bimetallic nanocatalysts can be increased [51,52]. The inclusion of additional metal changes the electronic configuration thereby creates ligand and strain effects. However, this needs to be yet fully understood to take advantage of bimetallic nanoparticles. The catalytic activity of bimetallic catalysts can be improved in several ways, one of which is charge transfer phenomena that alters the binding energy and reduces the obstacles for specific chemical reactions [53]. It also provides a shield from catalyst poisoning and catalytic deactivation [54]. There are a number of advantages of changing composition; it reduces the poisoning effect, and creates a new reaction pathway leading to a distinct selectivity. Furthermore, it might also generate a synergistic effect which alters the electronic configuration and thus improves the catalytic activity. Alloy and bimetallic nanocatalysts also can enhance the thermal stability in certain chemical reactions [52].

1.3.4. Surface area and Porosity

The catalytical activity of supported bimetallic catalysts is affected to a considerable extent by their surface area and porosity. These properties are also considered to be linked to creating a high dispersion of active catalyst components [1,3]. There are a number of studies existing on exploring the

effects of porosity and surface area on metal dispersion and their subsequent effect on the catalytic performance of bimetallic catalysts. It needs to be reflected here that it is hard to separate the influence of surface area from that of the surface chemistry. There are two ways of creating high surface areas, one is by making small metal particles where the surface area to volume ratio of single particles is high and the second way is to develop materials where the void surface area (pores) is large in comparison to the bulk carrier material. Highly dispersed supported metal catalysts and gas phase clusters can be considered relevant to the first method described above whilst the second group involves microporous materials such as amorphous silicas, zeolites, inorganic oxides, and porous carbons. There is a strong correlation between surface area and the pore size and the pore volume, i.e., if the pore volume is big the surface area is big and if the pore size is small the surface area is large. Surface area larger than that created by particle size reduction can result from porosity generation, particularly if the pores are small. There are two reasons why the concept of the surface area of a micro porous material is ambiguous. Firstly, there are a number of sound and innate definitions available for the molecular surface, which can yield significantly altered results under particular conditions; however, it remains not fully defined. Second the roughness of the surface must be accommodated once it has been selected. On the atomic scale, all surfaces are very corrugated leading to higher than expected surface areas, using microscopic definitions and this is an ongoing and continuous problem as compared to simulated and experimental results on porous materials.

2. Preparation and Characterization Methods of Bimetallic Catalysts

2.1. Preparation Methods

The synthesis methods of supported bimetallic nanoparticles (SBN) can have a clear impact on the catalytic properties of bimetallic catalysts and thus their catalytic activities. Supported bimetallic catalysts are prepared by different preparation methods such as impregnation, deposition-precipitation (DP), vapor deposition (VD), co-precipitation (CP), and liquid preparation methods. Such methods are briefly described in the following subsection:

2.1.1. Impregnation Method

Impregnation is a widely used preparation method for the synthesis of heterogeneous bimetallic catalysts. The impregnation methodology is where the support is contacted with an aqueous metallic solution (single or multiple) and then oven dried and calcined under suitable thermal conditions. Two types of impregnation methods can be used, (i) based on the volume of metallic solution with respect to the pore volume of support, namely incipient wetness and (ii) wet impregnation using excess solvent. In the case of incipient wetness, the active component solution volume is equal to the pore volume of the support and in the case of the wet impregnation methodology the volume of solution is much higher than the total pore volume of the support [55]. Temperature of stirring, time of heating, calcination temperature, and the nature of supporting material are some of the crucial conditions that control the characteristics of the final catalyst. Chemical reaction between the precursor solution and the metal support may occur during the calcination phase of the period, under particular conditions causing various active phase-support interactions. The advantage of this method is that highly dispersed metal particles on the surface of metal oxides (as supports) can be obtained.

2.1.2. Deposition-Precipitation Method

Deposition-precipitation (DP) technique is one of the most successfully used methods in order to obtain high dispersion and homogeneous deposition of bimetallic particles on the surface of the support. The DP method is used where the solution creates an insoluble form of supported active phase, and this in turn accumulates in the solution connected to the support. Strong precursor-support interactions are expected using this method which enhances the catalyst efficiency and stability of the catalyst. In this method the metal salts precursors are typically carried out in solution in the

presence of a suspension of the support by increasing the pH value in order to obtain immediate precipitation of different metals. For instance, this method is a widely used methodology for creating precursors of highly active supported gold catalysts [56]. Hydroxides or carbonates are created using this methodology and they accumulate on the support [57].

2.1.3. Chemical and Physical Vapor Deposition Methods

These two deposition methods are also important synthesis routes that are normally used for preparation of multicomponent or bimetallic nanoparticles. The synthesis of bimetallic catalyst can be obtained by either chemical or physical vapor depositions. For instance, chemical vapor deposition (CVD) is a reliable technique and relatively simple and implemented under mild conditions. On the other hand, physical vapor deposition (PVD) requires solid materials to be evaporated into supersaturated vapor, which supports the homogenous nucleation of metal particles in order to prepare SBN. Metal precursors, metal vapor nucleation, temperature, and type of gas are very important factors for synthesizing an efficient bimetallic catalyst using VD methods.

2.1.4. Co-Precipitation Method

Generally metal ions are soluble in acidified aqueous solution and they precipitate as their hydroxides, oxy-hydroxides, which upon calcination lead to the formation of suitable metal oxide phases. A mixed oxide in solid-solution form is generated by the co-precipitation of base metal cations. Co-precipitation of bivalent cations in the form of hydroxy-carbonate, hydroxyl-chloride or hydroxyl-nitrate is generated by precipitating hydrotalcite of bivalent cations [58]. This process usually produces contamination of the precipitate in the final product and this is restricted through a complex process of washing.

2.1.5. Liquid Preparation Method

This method, the most ancient and widely used chemical method for synthesis of nanoparticles, is by reduction of bimetallic ions in solution. In this method, bimetallic ions are reduced by providing some extra energy and using different types of chemical reductants. The provided energy is used to decompose the material, and usually, photo energy, electricity or thermal energy used. It is the most frequent chemical method used for the production of stable bimetallic nanoparticles. The advantage of this method is the ability to control the size of the bimetallic nanoparticles. This process is normally operated at low temperature, automatically reducing the production costs of large amounts of bimetallic catalysts [59]. For instance, the synthesis of colloidal bimetallic nanoparticles containing gold can be achieved using this method. Also, metal ions of bi- or tri-metals can be reduced by a suitable reductant such as citrate [60].

2.1.6. Catalyst Synthesis of Pd and Au Based Bimetallic Catalysts and Their Catalytic Testing Procedure

It should be noted that, unless otherwise mentioned, all reagents were obtained from Sigma-Aldrich (Merck KGaA, Darmstadt, Germany) and were applied without further purification.

Synthesis and Testing Procedure for Pd Based Catalysts

The catalyst synthesis recipe described below leads to solids used for the catalytic acetoxylation runs described in Section 3.1. The preparation of Pd based bimetallic catalyst involves mainly two steps: Step 1 involves the impregnation of commercial TiO_2 (anatase) with an aqueous solution of $SbCl_3$ by taking 8 wt % Sb with respect to the total amount of the catalyst and soaking for 1 h followed by precipitation with $(NH_4)_2SO_4$ and keeping at 70 °C for 1 h on a water bath. After cooling to room temperature, the solution is neutralized with ammonia (adjusted to pH of 7) and heated on a water bath for another hour. Afterwards the slurry is filtered and dried on a rota-vapor to remove excess of water: the resulting solid mass is further dried in an oven at 120 °C for 16 h, followed by calcination at

400 °C for 3 h in air (50 mL/min). Step 2 deals with the impregnation of the above-mentioned Sb/TiO_2 sample with the necessary amount of acidified aqueous solution of $PdCl_2$ to get the required amount of Pd. The solvent is removed by rota-vapor and the sample dried in an oven at 120 °C for 16 h. In the first case, the loading of Pd varied in the range from 0.5 to 20 wt % with constant Sb loading (8 wt %). In the second case, 10 wt % Pd was kept constant while the Sb content was varied in the range from 4 to 20 wt %. About 5 grams of each catalyst was prepared using this synthesis procedure.

Acetoxylation runs were performed in a continuous fixed bed, vertical and tubular stainless steel reactor (length: 112 mm; i.d. 6 mm). The reaction gases like synthetic air (20.5% O_2 in N_2) as oxygen source and Argon (99.999%) used as diluent gas were supplied from commercially available compressed gas cylinders and used without further purification. The flow rates of these gases were measured using mass flow controllers. About 1 mL (ca. 0.8 g) of catalyst particles (0.425–0.6 mm size) was loaded into the reactor and activated in an airflow of 27 mL/min at 300 °C for 2 h prior to each activity measurement. The organic feed mixture of toluene and acetic acid was pumped to the reactor using an HPLC pump (Shimadzu GC 8A, Overland Park, KS, USA). The liquid reactant mixture was vaporized before entering the reactor in a preheating zone provided on the top of the reactor. The molar ratios of all the reactants such as toluene:acetic acid:oxygen:inert gas were 1:4:3:16. The reactor was heated up to reaction temperature in an Ar-stream. After reaching reaction temperature, a mixture of air, argon, and vaporized liquid substrates was introduced and the reaction was carried out at a temperature of 210 °C and at a pressure of 2 bar. The product stream was analyzed on line by gas chromatography (GC, HP-5890) using a HP-5 capillary column (50 m × 0.32 mm) and FID detector. The column outlet was connected to a methaniser (30% $Ni\text{-}SiO_2$ catalyst), which converts all the carbon-containing products, including CO and CO_2 into methane.

Catalyst Synthesis and Catalytic Testing Procedure for Au Based Catalysts

Catalyst preparation involved two steps. In the first step, $HAuCl_4$ was dissolved in 60 mL distilled water. In the second step, the required amount of $PdCl_2$ solution (M) was dissolved in 10 mL of distilled water. This solution was heated to 50 °C for 10 min and a few drops of HCl were added to completely dissolve the $PdCl_2$ precursor. The solution was then added to the gold chloride solution that was prepared in the first step followed by the reduction of the bimetallic solution using a mixture of 1% tannic acid and 1% of sodium citrate under stirring at 60 °C. After that, the resulting materials from step-1 and -2 were deposited onto the chosen oxidic support (e.g., anatase TiO_2). Afterwards, the resulting slurry was stirred for 2 h at r.t. and then the excess solvent was removed using a rotary evaporator. The obtained solid was oven dried at 120 °C for 16 h and then calcined at 350 °C for 5 h in air. In a similar way, another metal such as Ag was doped separately as the second metal using a similar preparation method. Besides two bimetallics ($AuPd/TiO_2$ and $AuAg/TiO_2$), three monometallic catalysts, Au/TiO_2, Pd/TiO_2 and Ag/TiO_2, were also prepared and conditioned in a similar way.

Catalytic tests were carried out under pressure using a Parr autoclave (100 mL) according to the procedure described below. In a typical experiment, the reaction mixture consists of 0.3 g of supported metal catalyst, 5 mL of cyclohexane (CH), 25 mL of acetonitrile as solvent, and 0.1 g of tert-butyl hydroperoxide (TBHP). These components were taken in an autoclave and flushed three times with O_2 before setting the initial reaction pressure of O_2 to 10 bar. Concerning the start-up procedure, this was performed with the O_2 line opened, and as the O_2 was consumed, it was replaced from the cylinder, maintaining the overall pressure constant. The stirring speed of the reaction mixture was set to 1500 rpm in general and the reaction was performed at 150 °C for 4 h unless otherwise stated. At the end of the reaction, the solid catalyst was separated by centrifugation. Products were collected at different intervals and analyzed by gas chromatography (Agilent 6890 N).

2.2. Characterization of Bimetallic Catalysts

A comprehensive knowledge of the chemical and physical properties of bimetallic nanoparticles as heterogeneous catalysts is needed to understand the nature of active sites, which in turn can help to find and tune the key performance indicators. It is essential to understand the catalytic behavior of these materials including deactivation phenomena in such a way that their performance can be further improved. More profound insights on the metal particle structure, size, shape, and catalytic properties of the materials can be gained through a range of methodologies that can be used to categorize them. A range of characterization techniques for identification and characterization of the bimetallic catalysts are illustrated in Figure 3 and the information obtained from these techniques is used for their classification. These techniques can be used either individually or collectively applied in order to understand and analyze the properties of SBN. The data outlining the structural properties can be given by a range of methods such X-ray diffraction, UV-vis (Tokyo, Japan), and vibrational spectroscopy, neutron and electron diffraction methods etc. The list of characterization methods and the information that can be obtained from these techniques are illustrated in Figure 3. X-ray fluorescence (XRF), atomic absorption spectroscopy (AAS), inductively coupled plasma (ICP) (Waltham, MA, USA), and energy-dispersive X-ray (EDX) (Tokyo, Japan) are some of the other methods that can provide the elemental composition. The magnitude and morphology of the bimetallic catalysts can be better understood by utilizing a range of different kinds of microscopy methods (e.g., TEM and SEM) (Tokyo, Japan). The surface structure and composition of bimetallic catalysts can be illustrated using spectroscopic methods (e.g., Raman and X-ray photoelectron (XPS)) (Eden Prairie, MN, USA).

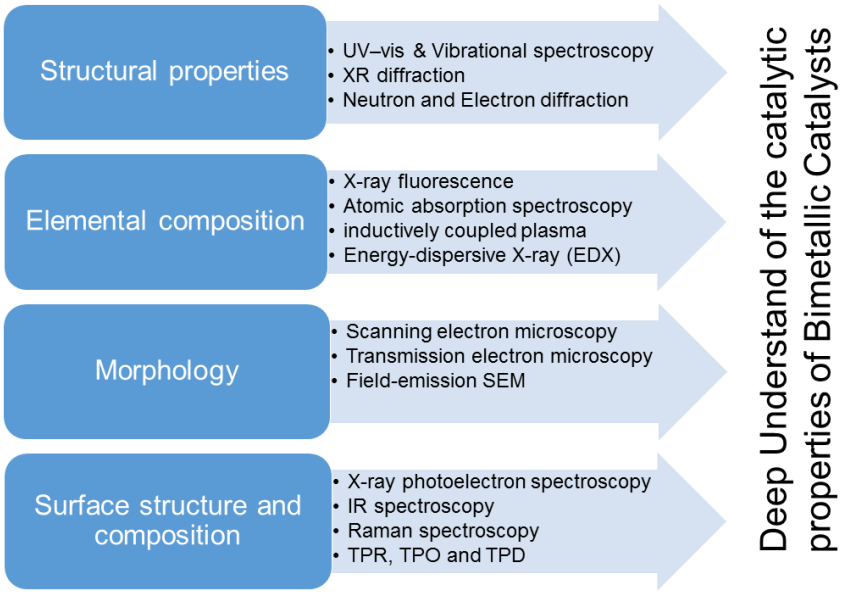

Figure 3. Summary of some selected characterization methods of bimetallic catalyst.

A number of characterization methods are outlined and discussed below. Transmission electron microscopy (TEM) is a very popular technique used for the structural characterization of bimetallic nanoparticles [61,62]. The computation of the chemical composition of nanoparticles is derived from information on lattice spacing provided by high-resolution TEM. Particle size, shape, and distribution can be determined from TEM. Crystallographic planes are worked out by measuring the scattering of the electron beam which also provides information about phase and crystallinity of bimetallic nanoparticles. Scanning TEM by energy dispersive spectroscopy is an alternative technique used to know the chemical composition of particles. Here a narrow beam of electrons is focused on a small area on the sample, the energy of the X-rays emitted from the nanoparticles is recorded, and electron energy losses are measured as a spectrum display and then used to correlate the image with quantitative

data [63]. This technique was applied by Wu Zhou et al. to characterize the supported metal oxide and to locate the active sites of the catalyst [64]. Electron microscopy was used by Akita et al. in their study of the morphology of gold nanoparticles [65].

The crystallographic structure and phase composition can be found by X-ray diffraction (XRD) (Darmstadt, Germany) [66]. There are three main components of an XRD, a beam source, a goniometer, and a detector. Bragg's law tells us that X-rays are diffracted from material at a specific angle, and this diffraction can be used to determine the composition of the material and also used to find the size of the crystal using the Scherrer equation as well as distinguishing the characteristics of the random and ordered alloys. Different packing structures like FCC and BCC exist in different alloys and each one gives different diffraction patterns [67]. The outputs from an XRD patterns can be compared against database patterns which are retained in the International Center for Diffraction Data (ICDD). For exact measurement and positioning of atoms in complex structures Rietveld analysis is used. In severe environments such as very high temperature and during chemical reactions XRD can be used [68].

The electronic structure of bimetallic nanoparticles can be characterized using the UV-vis method which reveals the electronic absorption in the UV and visible regions [69,70]. The basis of this technology is that electron conductors absorb near the UV and visible region whilst semiconductors absorb in the UV and visible region so this method is mostly used for powder samples, providing information about the electronic properties in the coordination and oxidation states. Data regarding the structure of both amorphous and crystalline bimetallic nanoparticles can be obtained using vibrational spectroscopy technology such as infrared spectroscopy and Raman spectroscopy [71,72]. In their research on M-CO bonding using this technique, Bao et al. [73] were able to isolate the active surface of nanocatalysts inside carbon tubes. The structural properties of nanoparticles of Rh and Pt using vibrational spectroscopy were investigated by Somorjai et al. [74].

The surface composition, oxidation state etc. of bimetallic catalysts can be found using X-ray photoelectron spectroscopy (XPS), where the photoelectric effects existing on the surface of solid nanoparticles cause the electrons belonging to the nanoparticles to become excited and escape into the vacuum [75]. The binding energy of the electrons is computed using the energy of the photoelectron and this is dependent on oxidation so it also provides the data on oxidation states [75].

The composition of elements can be identified using X-ray fluorescence (XRF), here X-rays created by accelerating the electron in the metal using high potential charge, are emitted during the jump of an electron from a higher to a lower level. The material absorbs the primary X-rays and this precipitates the movement of an electron from one level to another level at the same time emitting secondary X-rays, which give data on the chemical composition of the material. Information on catalytic poisoning can also be gained by calculating the elemental deposition of elements such as chlorine or sulfur. The particular benefit of this technology is that sample preparation is not a requirement.

3. Own Results

3.1. Palladium Based Bimetallic Catalysts

It is known that catalysts having more than one metal can exhibit superior catalytic properties to monometallic catalysts due to generation of bi- and multi-functional properties owing to synergistic effects between the components present in the catalyst composition. Our own results have clearly displayed such amazing synergistic effects in the vapor phase toluene (Tol) acetoxylation to benzyl acetate (BA) reaction (Scheme 1).

The first studies of our investigations were dedicated to Pd based catalysts and checked their potentiality towards acetoxylation of toluene. Scheme 1 compares the commercial route for producing BA, involving the multi-step process with that of our one-step approach. In addition, the commercial process also involves chlorine chemistry and hence is environmentally unfriendly. On the other hand, the present acetoxylation is a simple and single step process besides its eco-friendly nature. The desired product is benzyl acetate while other by-products such as benzaldehyde (BAL), CO_x and H_2O are

also formed in smaller proportions. In addition, this direction also gives the chance of making benzyl alcohol (BOL) by simple hydrolysis of BA. BOL has a huge market compared to BA. On the other hand, it is very difficult to produce BOL from toluene directly in one-step.

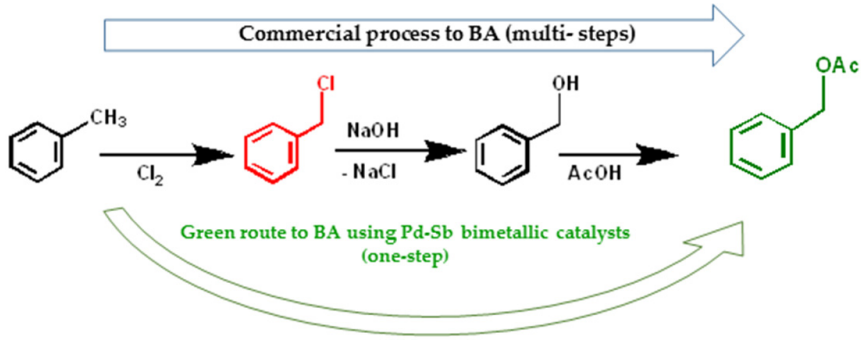

Scheme 1. Comparison of commercial process for benzyl acetate (BA) production with that of one-step gas phase acetoxylation route using Pd-Sb bimetallic catalysts.

It should be noted that the catalysts used in this study were prepared by a wet impregnation method [76]. It is evident from Figure 4 that the catalytic results obtained on monometallics were inferior compared to bi-metallic Pd-Sb catalysts. It is also obvious that pure TiO_2 support is almost inactive, as expected and in a similar manner, monometallic 8% Sb/TiO_2 catalyst displayed much lower catalytic activity, i.e., X-Tol $\leqslant$ 2%. The most striking feature here is that presence of both Pd and Sb which revealed substantial effect on the catalytic performance. In other words, the combination of Pd and Sb totally improved the direction of reaction in the desired way. Consequently, the yield of COx remarkably reduced from >50% to below 5%. Quite interestingly, the yield of BA significantly enhanced from ca. 2% to >30%. In addition, the conversion of acetic acid (X-AcOH) also reduced from 54% to ca. 35% indicating a considerable decrease in the combustion reaction that leads to the formation of CO_x. Such enhanced performance of bimetallic Pd-Sb catalyst is undeniably due to existence of synergistic effects between the two metals (i.e., Pd and Sb). These results clearly emphasize the need for the 2nd metallic component to enhance the catalytic performance. After such an amazing effect of the 2nd component, we tried a variety of promoters (instead of Sb), supports, optimisation of Pd and Sb contents etc. Such results are discussed below one after the other in a systematic way.

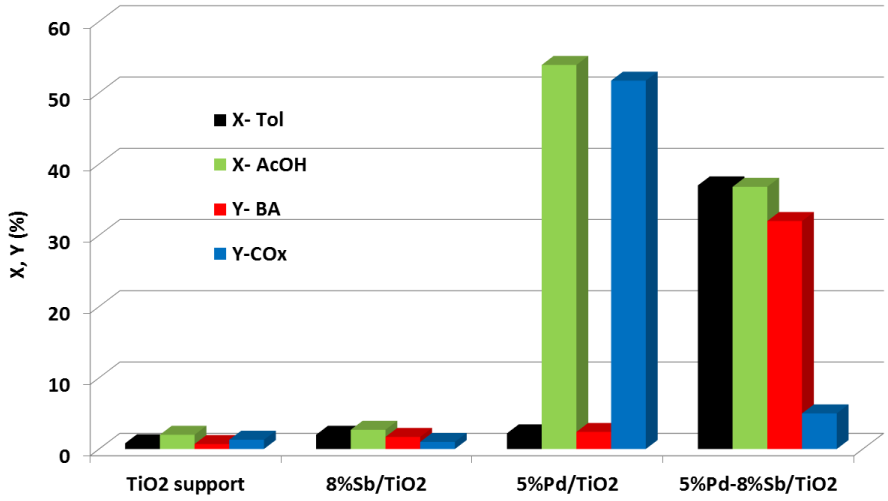

Figure 4. Synergistic effects between Pd and Sb in Pd-Sb/TiO_2 catalyst in the acetoxylation of toluene to benzyl acetate (Reaction conditions: Tol:AcOH:O_2(air): Ar = 1:4:3(15):4; GHSV = 2688 h^{-1}; τ = 1.34 s; T = 210 °C; P = 2 bar). GHSV: Gas hourly space velocity.

Effect of promoter on the activity and selectivity of Pd-M/TiO_2 catalysts (M = Sb, Bi, Sn, Cu) in toluene acetoxylation is shown in Figure 5 [76].

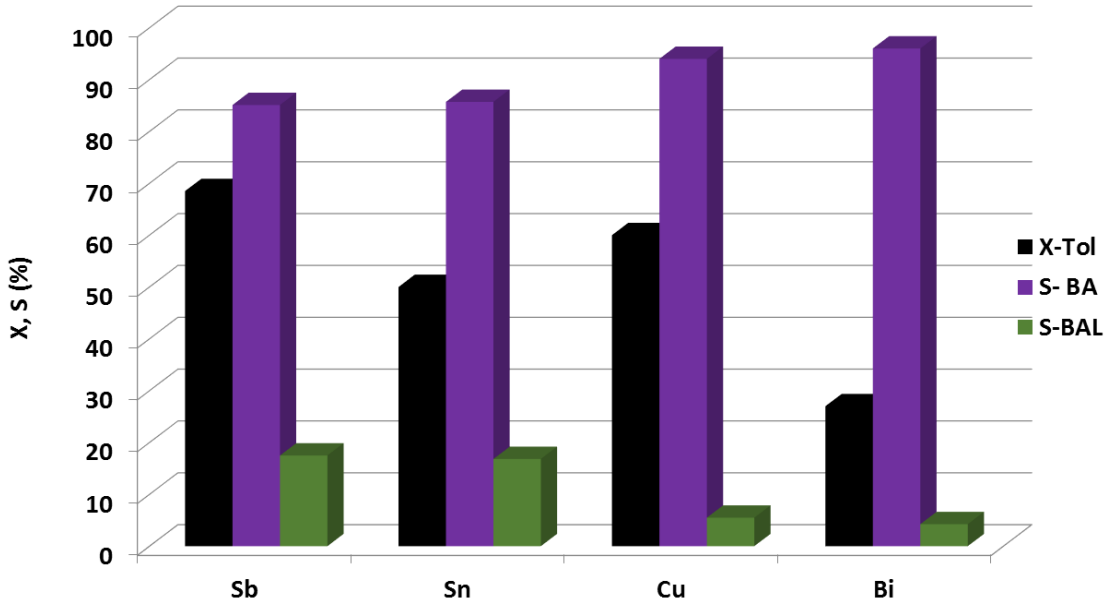

Figure 5. Effect of promoter on the catalytic performance of 10% Pd-8% Sb/TiO_2 catalyst. (Reaction conditions: Tol:AcOH:O_2(air):Ar = 1:4:3(15):4; GHSV = 2688 h^{-1}; τ = 1.34 s; T = 210 °C; P = 2 bar).

It can be seen that the nature of the promoter has a substantial influence on the catalytic performance. Among the four different promoters investigated, Sb was found to be the best in terms of conversion of toluene. Even though, low conversion of toluene is achieved using Bi as a promoter, it shows another beneficial effect on the long-term stability of the catalyst. Pd-Sb catalysts despite higher activity are used to undergo easy deactivation. On the other hand, Bi and Cu promoted catalysts could solve this problem of deactivation by means of reduced coke deposition and by altering the nature of coke deposition [77,78]. After identifying the higher activity of Pd-Sb/TiO_2 catalyst, the optimization of both Pd and Sb contents was further explored in subsequent efforts. For this purpose, two different types of catalysts were prepared by varying the contents of Pd and Sb. In the first series, we kept the Sb loading constant (8 wt %) and changed the Pd loading over a wide range (0.5 to 20 wt %), while in the second series, we kept the Pd content (10 wt %) constant and changed the Sb loading from 4 to 20 wt %. The results of these two series are discussed below. Figure 6 demonstrates that an increase in Pd content has clearly improved the conversion of toluene from 16% to >90% with an increase in Pd content from 0.5 to 20 wt %. However, the conversion of toluene is found to increase at a faster rate up to a Pd loading of 10 wt % and at a slower rate beyond this loading. The BA selectivity is not altered to a considerable extent and remains nearly constant at ca. 85%. In other words, the selectivity of BA is independent of the conversion of toluene. This fact suggests that the product, BA, appears to be a quite stable end product under the reaction conditions applied and hence does not undergo any consecutive reactions to give unwanted by-products. As a result, the BA yield improved considerably and reached a value close to 80%.

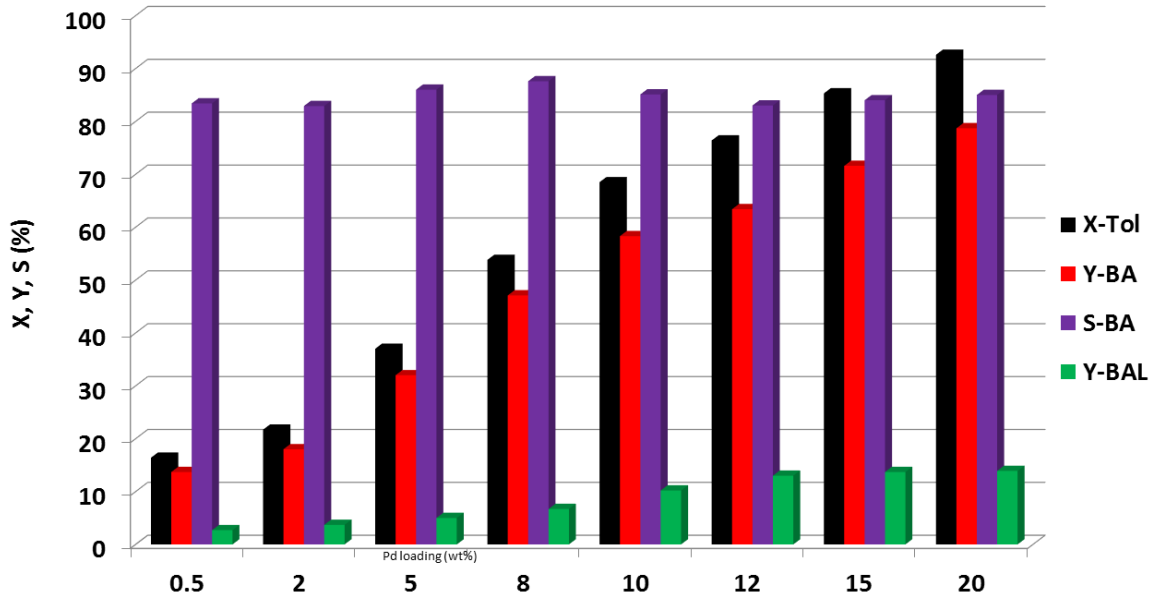

Figure 6. Effect of Pd loading on the catalytic performance of *x*Pd-8% Sb/TiO_2 catalyst (Reaction conditions: Tol:AcOH:O_2(air):Ar = 1:4:3(15):4; GHSV = 2688 h^{-1}; τ = 1.34 s; T = 210 °C; P = 2 bar) [79].

As mentioned earlier, benzaldehyde (BAL) is the major by-product and the balance is total oxidation products. The selectivity to benzaldehyde (S-BAL) varied in the range from 10% to 15%. The higher conversions and greater yields were obtained at higher Pd contents, which might be due to formation of bigger Pd particles (as evidenced from TEM). The peculiar property of this reaction is that bigger Pd particles are more active and selective compared to small Pd particles. Among all, 20 wt % Pd displayed the superior performance. However, due to the expensive nature of 20 wt % Pd, we selected 10 wt % Pd as the model catalyst and used it further in subsequent experiments. Despite achieving an acceptably higher conversion of toluene and high yield of BA, the catalyst samples were observed to suffer from the problem of easy catalyst deactivation. The analysis of coke in the spent (deactivated) samples indicated that the deactivation was due to carbon deposits during the course of the reaction [79]. The amount of coke deposition was observed to increase with increasing Pd load. The highest amount of coke expected, for instance, in the deactivated 20 wt % Pd content catalyst is 7.3%. However, this type of catalyst can be regenerated in air (at 250 °C for 2 h) and can be applied again for more cycles with constant catalytic activity. After identifying the optimum loading of Pd, further efforts were focused on optimizing the Sb content.

It is clear from Figure 7 that the content of Sb also matters a lot. The toluene conversion is found to improve with Sb loading (up to 8 wt %) and then decrease with further increase in Sb content beyond 8 wt % [80]. However, the selectivity of BA was found to remain more or less constant at around 85% throughout irrespective of Sb loading. Among all, 8 wt % Sb seemed to be optimum for enhanced performance. After testing these two series of catalysts, one concluded that 10% Pd and 8% Sb on TiO_2 (anatase) was the right combination and hence this was used as a model catalyst in the next runs. Besides Sb, the influence of various other co-components (e.g., Au, Mn, Co) was also investigated and characterized by X-ray absorption spectroscopy (XAS) in order to elucidate the nature of co-components and their impact on the catalytic activity/selectivity [81]. It was observed that Mn and Co oxides spread on the support TiO_2 surface while Au forms separate small metal (Au) nanoparticles besides Pd particles and exhibits a different influence on the catalytic performance.

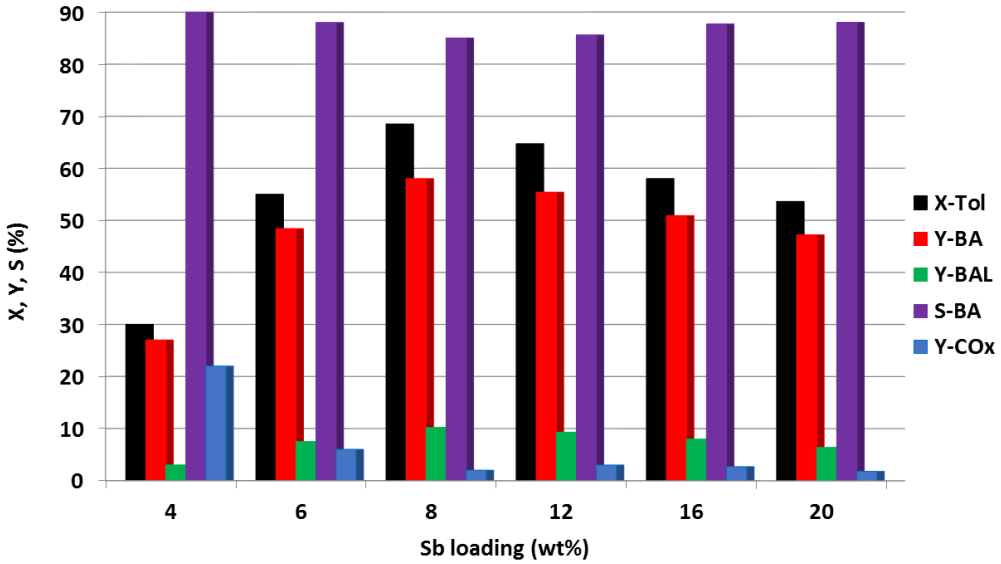

Figure 7. Effect of Sb loading on the catalytic performance of 10% Pd-*x*% Sb/TiO_2 catalyst (Reaction conditions: Tol:AcOH:O_2(air):Ar = 1:4:3(15):4; GHSV = 2688 h^{-1}; τ = 1.34 s; T = 210 °C; P = 2 bar) [80].

Figure 8 illustrates that the kind of support used revealed a significant effect on both the catalytic activity and/or selectivity of the solids. Among, four different supports investigated, TiO_2 anatase support was found to be the best in terms of conversion of toluene and selectivity of BA. However, the lowest activity and the highest CO_x (ca. 30%) were observed using ZrO_2 and Al_2O_3 as supports (*X* – Tol = ~10% and *Y* – BA = ~8%). On the whole, the activity and selectivity behavior of catalysts supported on different metal oxides is related to the size of Pd particles formed in them and the growth mechanism of Pd (e.g., surface reconstruction) during the course of the reaction. One can clearly see big differences in the Pd particle size, particle composition, and coke deposition, which strongly depended upon the nature of support used. About a decade ago, Shu et al. [82] investigated the gas-phase acetoxylation of toluene with acetic acid to benzyl acetate using Pd-Sn-K/SiO_2 catalysts and claimed relatively low toluene conversion of 25% with ca. 90% selectivity of benzyl acetate. Additionally, Komatsu et al. [83] also used different Pd-containing bimetallic catalysts for the present acetoxylation of toluene to benzyl acetate.

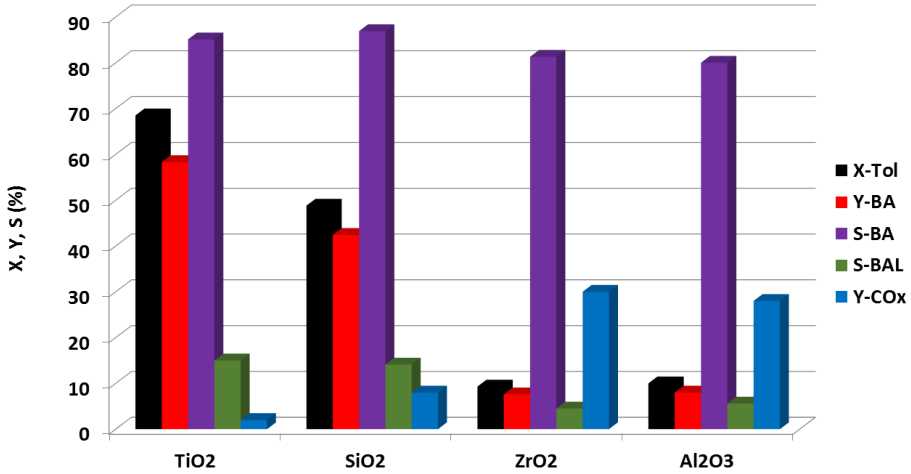

Figure 8. Effect of kind of carrier on the catalytic performance of 10% Pd-8% Sb/support catalyst (Reaction conditions: Tol:AcOH:O_2(air):Ar = 1:4:3(15):4; GHSV = 2688 h^{-1}; τ = 1.34 s; T = 210 °C; P = 2 bar).

As mentioned above, these catalysts undergo deactivation during time-on-stream (i.e., after several hours of operation). In order to explore the changes occurring at different stages of the reaction and also to identify the reasons for such deactivation, the catalyst subjected to four different stages was collected. The catalyst samples were collected at four different stages such as (i) immediately after activation in air (A); (ii) maximum active one (MA); (iii) deactivated one (DA) and (iv) after regeneration (R). Due to superior performance of 10% Pd-8% Sb/TiO_2 solid, this particular catalyst was selected for such a study and characterized by X-ray Photoelectron Spectroscopy (XPS). The results of this XPS study are depicted below in Figure 9 with respect to the proportion of different Pd species existing in the near-surface region. It is quite evident from the figure that the activated sample (i.e., after the activation at 300 °C/2 h/air) contains exclusively (100%) oxidized surface Pd species, as expected. In the catalyst when it reaches maximum activity, the catalyst surface consists of both metallic Pd (65%) and the oxidized Pd species (i.e., 35% PdO species). Quite surprisingly, no such oxidized Pd surface species exists in the deactivated catalyst, instead, it contains both metallic Pd(0) and $Pd^{\delta-}$ species. However, the regenerated catalyst, which immediately restored maximum activity, contains a major proportion of oxidized Pd (i.e., PdO) species due to removal of coke during such an oxidative regeneration procedure in air. It is also worth mentioning that even though three different surface species exist in these samples; all the three species were never present together in any one sample at any stage of the reaction. Our results also provide hints that the formation of $Pd^{\delta-}$ species with lower binding energy values of Pd electron compared to metallic Pd is the more probable reason for the deactivation of the catalysts [73]. Formation of such a species is expected from the strong interaction between metallic Pd and the carbon species from the coke deposits.

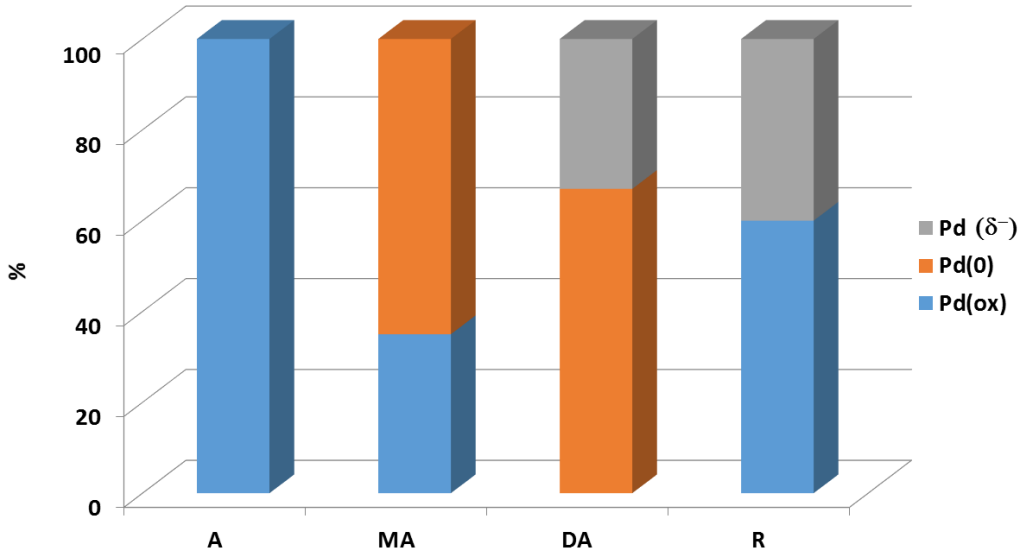

Figure 9. Different Pd species on the surface of 10% $PdSb/TiO_2$ catalyst at different stages of reaction (A: activated; MA: maximum active (X = 68%, after 11 h operation); DA: deactivated (X = 46%, 22 h); R: regenerated (X = 68%)).

3.2. Gold Based Bimetallic Catalysts

In the initial stages, we explored the impact of five different oxide supports on the catalytic performance of monometallic Au nanoparticles. Bimetallic catalysts including Au-Pd and Au-Ag loaded on TiO_2 were synthesized using a colloidal impregnation method and then their catalytic activities were investigated using similar metal contents, i.e., 1 wt % Au and 1 wt % second metal. To understand the properties of these catalysts, different characterization methods were applied. BET surface area (Micromeritics, Norcross, GA, USA), pore volumes and ICP values of such catalysts are summarized in Table 1.

Table 1. BET surface areas and inductively coupled plasma (ICP) results of Au-bimetallic (1 wt % each) catalysts over TiO_2 (anatase).

Entry	Catalyst	Catalyst Composition (ICP)		BET-SA (m^2/g)	Pore Volume (cm^3/g)
		Au (wt %)	Pd/Ag (wt %)		
1	Au/TiO_2	0.9	-	43	0.12
2	Pd/TiO_2	-	1.0	55	0.80
3	Ag/TiO_2	-	1.0	39	0.90
4	$AuPd/TiO_2$	1.1	1.2/-	38	0.071
5	$AuAg/TiO_2$	1.2	-/1.2	31	0.057

ICP results showed that nominal and actual loading of bimetallic catalysts were comparable values (0.9–1.2 wt % Au, Pd, and Ag). The BET surface areas and pore volumes were observed to change considerably by changing the type of metal. Au and Pd nanoparticles supported on TiO_2 displayed somehow a higher surface area and pore volume compared to $AuAg/TiO_2$.

The XRD patterns of the bimetallic catalysts are presented in Figure 1. It is obvious from Figure 10 that there are no reflections belonging to either the Au or the Pd metallic phases. This is due to their low concentrations (1 wt %) and also due to their X-ray amorphous nature, probably. We assume that the particle size of metal nanoparticles appeared to be too small to be identified using XRD. Such results are found to be in good agreement with TEM results where the particle sizes of these metals are small. As shown in Figure 10, we can clearly see the reflections corresponding to TiO_2. However, TiO_2 supported 1%Au-1%Ag catalyst, exhibited a very weak reflection corresponding to the Au metallic phase besides the typical TiO_2 (anatase) reflections.

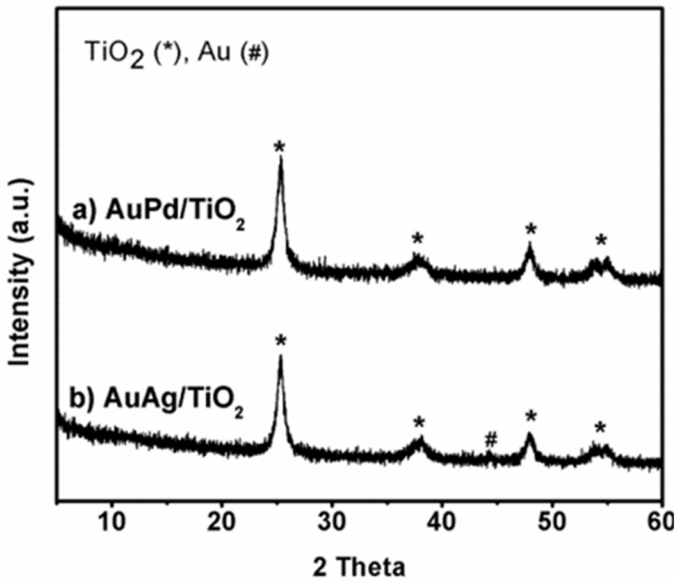

Figure 10. XRD patterns of different bimetallic catalysts (**a**: $AuPd/TiO_2$; **b**: $AuAg/TiO_2$).

Furthermore, the catalytic activity of supported metals nanoparticles (e.g., Au, Pd, etc.) is strongly dependent on its particle size; TEM studies were conducted to explore the properties of supported bimetallic catalysts. As shown in Figure 11, our bimetallic catalyst displayed a narrow size particle distribution (inset of Figure 11a,b) but varying size of metal particles. The TEM image of Au-Pd (Figure 11a) shows that the particles supported on TiO_2 are almost spherical with an average size of 1 to 5 nm. Conversely, the size of Au-Ag nanoparticles supported on TiO_2 (Figure 11) showed to some extent bigger particles compared to the Au-Pd catalyst, which vary between 2 nm and 9 nm. Interestingly, the lattice spacing calculated from the HRTEM for Au-Ag supported on TiO_2 (Figure 11d) shows a value of about 0.230 nm, which lies between the Ag (111) plane (0.226 nm) and the Au (111)

plane (0.235 nm). Furthermore, the corresponding EDX patterns for some representative particles are shown in the insert images of Figure 11a,b of the Au-Pd and Au-Ag catalysts supported on TiO_2.

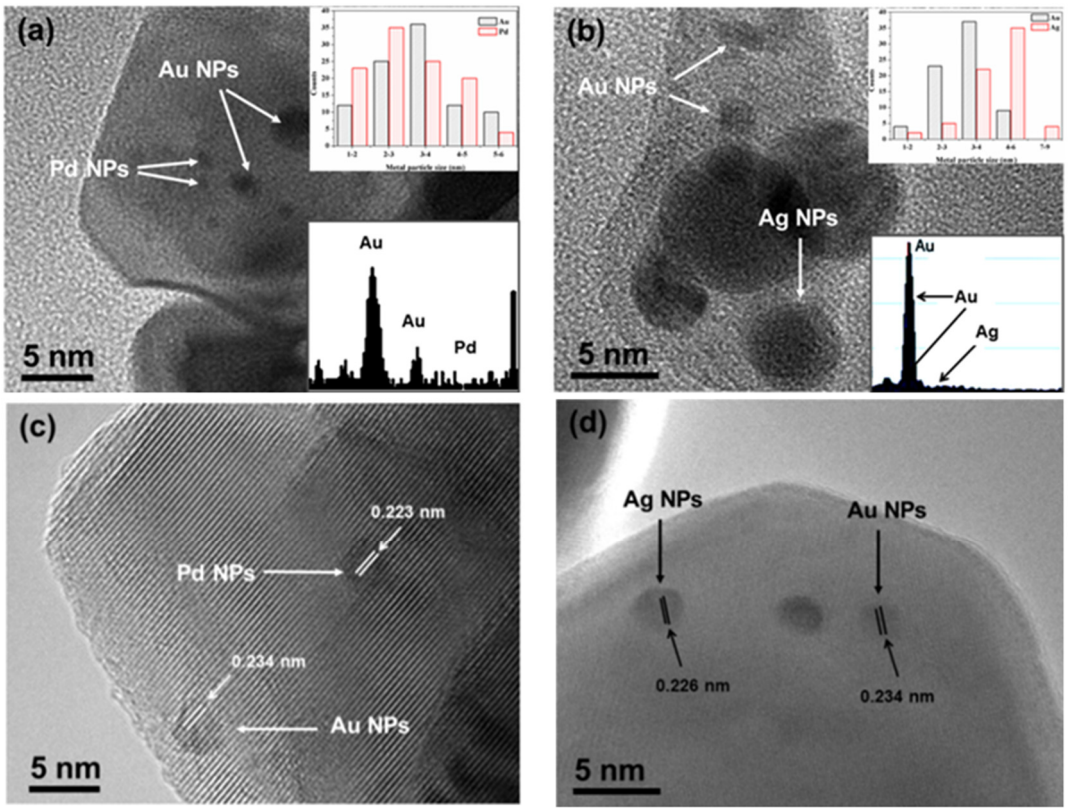

Figure 11. TEM (Transmission electron microscopy) (**a**: Au-Pd and **b**: Au-Ag) and HR-TEM (**c**: Au-Pd and **d**: Au-Ag) images of Au-Pd and Au-Ag catalysts supported on TiO_2 (anatase). EDX (energy-dispersive X-ray) spectra belong to AuPd/TiO_2 (inset **a**) and AuAg/TiO_2 (inset **b**) catalysts. Histograms show particle size of AuPd (inset **a**) and AuAg (inset **b**) supported on TiO_2 [84].

Using such catalysts, the possibility of producing adipic acid (AA) from the oxidation of cyclohexane (CH) in one-step was checked (Scheme 2). In these investigations, we were successful in showing a new path for the production of AA from CH. Besides AA, cyclohexanone (One); cyclohexanol (Ol) were also formed in considerable amounts. It was noticed that the nature of the support revealed a strong effect on the catalytic activity [85]. Among the five different supports applied, it was found that TiO_2 (anatase) showed the best performance while MgO showed a poor performance. From the best case, 26% conversion of CH and about the same selectivity of AA could be achieved. On the other hand, the sum selectivity of -One and -Ol amounts to roughly 70%. In subsequent studies, we extended such knowledge to check the effect of the 2nd metal (i.e., bi-metallic) on the conversion of CH and the selectivity of AA.

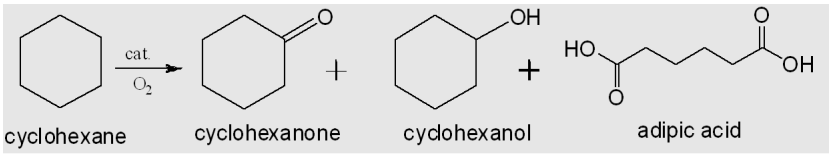

Scheme 2. Manufacture of adipic acid through the oxidation of cyclohexane.

A set of experiments was performed under identical reaction conditions in order to investigate the effect of the second-metallic element (i.e., bimetallic system) on the catalytic activities for the

production of adipic acid from cyclohexane by a one-pot oxidation reaction. For these tests, five different catalysts; pure TiO_2 support, monometallic systems such as 1% Au/TiO_2 and 1% Pd/TiO_2 as well as the bimetallic systems (1% Au-1% Pd/TiO_2) and (1% Au-1% Ag/TiO_2) were synthesized and evaluated in the direct oxidation of cyclohexane to adipic acid [84]. Such catalytic activity results are presented in Figure 12.

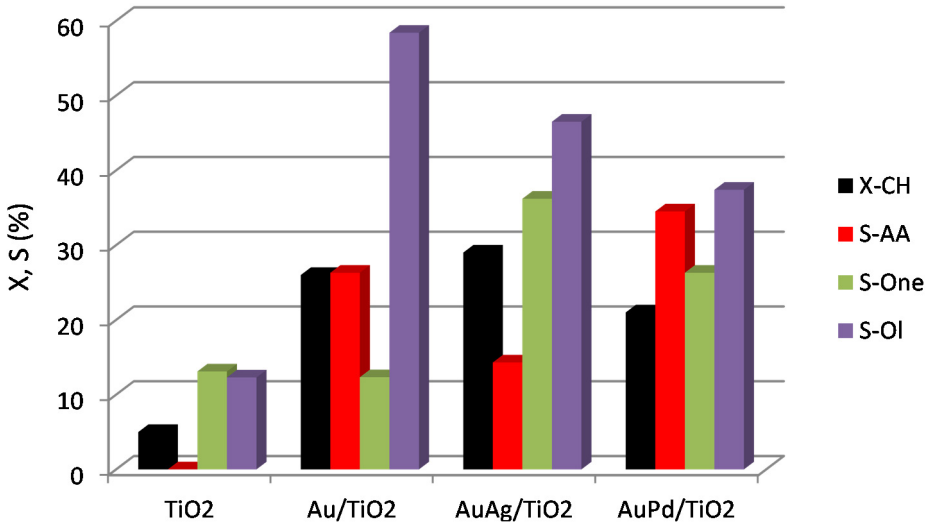

Figure 12. Effect of 2nd metal on the catalytic performance of Au-M/TiO_2 (M = Ag, Pd) catalysts for the oxidation of cyclohexane Reaction conditions: 5 mL CH, 25 mL solvent (acetonitrile), 0.1 g TBHP, T = 150 °C, P_{O2} = 10 bar, t = 4 h, 1500 rpm).

As expected, using the pure support (e.g., TiO_2) showed the poorest catalytic activity. However, impregnating gold nanoparticles to TiO_2 as monometallic catalyst improved the catalytic activity significantly (i.e., X-CH = ca. 25%, and S-AA = 26%). Furthermore, impregnating the Pd nanoparticles to TiO_2 (i.e., Pd/TiO_2 catalyst) displayed to some extent lower catalytic activity (X-CH = 16%, S-AA = 18%) compared to gold nanoparticles over TiO_2. Remarkably, the combination of the two metals nanoparticles (i.e., Au and Pd) as well as supporting them on TiO_2 obviously enhanced the selectivity of AA from 26 to ca. 34%, which is almost double the S-AA obtained on Pd/TiO_2 and also remarkably higher even when compared to monometallic Au/TiO_2 catalyst. Furthermore, the conversion of CH (X = 21%) obtained on bimetallic Pd-Au/TiO_2 was significantly higher than monometallic Pd/TiO_2 but slightly lesser than the monometallic Au/TiO_2 sample. Additionally, the Ag/TiO_2 has no appreciable influence on the activity and selectivity behavior compared to Au/TiO_2. Nevertheless, the catalytic performance of using Au-Ag/TiO_2 suggests that the presence of Ag has a clear influence on the catalytic activity but in a different direction compared to the Pd/TiO_2 system. Using Ag as the second metal, not only the selectivity to One + Ol (S = 82%) was considerably enhanced compared to all monometallic systems (Ag/TiO_2, Pd/TiO_2 and Au/TiO_2) but also the conversion of CH increased. Nonetheless, the influence of the presence of Ag nanoparticles has an impact on the yield of adipic acid. Considering all these effects, it can be claimed that the addition of the second metallic component has a clear promotional effect on the selectivity to AA, which might be due to the expected synergistic effects between Pd and Au and also the formation of small Au nanoparticles (AuNPs). However, the precise role of the second metal is still a matter of discussion, and hence, further studies are necessary for better understanding of the properties of bimetallic catalysts. Efforts were also made by different research groups to produce adipic directly from cyclohexane in one-step. However, those efforts were not really successful. For instance, Hereijgers et al. [86] studied the catalytic oxidation of cyclohexane over Au-based catalysts but they did not report the formation of any amounts of adipic acid from their investigations. In addition, the stability of the catalysts is an

interesting topic from both the industrial and environmental points of view. The stability of the tested bimetallic catalysts was conducted in reusable tests for a greater number of cycles to get knowledge of the long-term stability of the catalysts. The results of such investigations are illustrated in Figure 13.

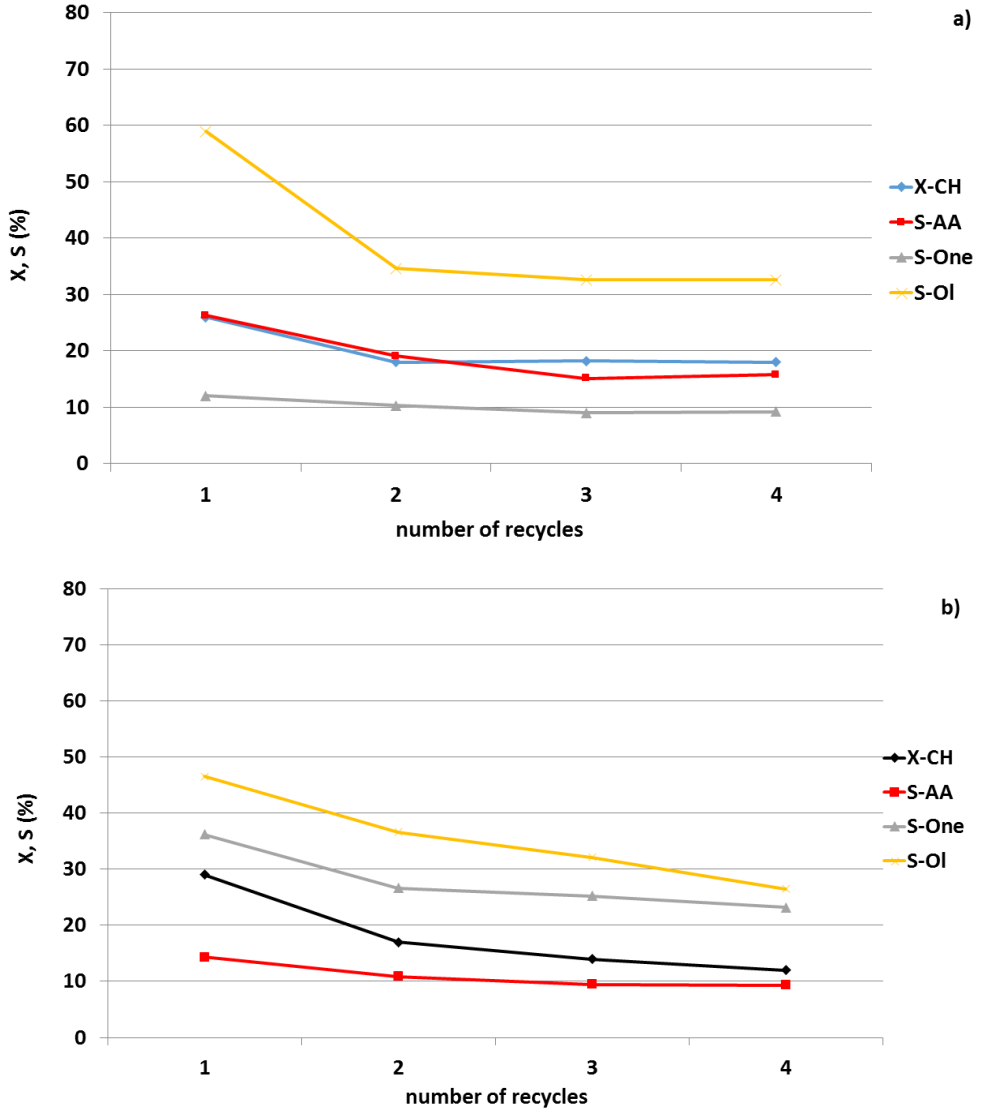

Figure 13. Recycling results of AuPd/TiO_2 (**a**) and AuAg/TiO_2 (**b**) catalysts for the oxidation reaction of cyclohexane (X—conversion, S—selectivity, CH—cyclohexane, AA—adipic acid, One—cyclohexanone, Ol—cyclohexanol; reaction conditions as in Figure 12).

The used bimetallic catalysts were filtered after the first run, and then washed, dried at 120 °C before conducting the second test following the same reaction conditions. Such steps were repeated four times to check the long-term stability of the catalysts. As shown in Figure 13, the conversion of CH and the selectivity of products after the first run over AuPd/TiO_2 catalyst decreased slightly. However, this catalyst displayed somehow good stability up to three runs. The selectivity to Ol also decreased from the first run to the second run and then remained more or less constant. On the other hand, a considerable decrease in the conversion of CH and the selectivity of products after four runs was observed in the case of using AuAg/TiO_2 catalyst. We can conclude from these results that AuPd/TiO_2 is more stable compared to AuAg/TiO_2 catalyst. The reasons behind such decrease in the catalytic activity after four cycles could be either due to the leaching of metal components or deactivation

by coke or due to marginal loss of catalyst weight during the work-up process of recovery of the catalyst [84].

4. Conclusions

Supported bimetallic nanoparticles (SBN) catalysts are an important class of heterogeneous catalysts due to their remarkable catalytic properties that are different compared to the individual metal components. Such types of materials have expanded a broad interest over a wide range of applications including catalysis. The provision of supporting these bimetallic nanoparticles has been established as an effective means of developing their versatility in a variety of environmentally friendly catalytic applications. What is of particular interest with respect to these bi-metals is their high surface area-to-volume ratio of solid-supported metal particles, which is fundamentally influential with respect to their catalytic characteristics. This review briefly presented the most important methods used to synthesis SBN, and what has become clear is that the applicability of each method is largely dependent on the purpose to which it is to be put. This review also shows the need for further research into SBN catalytic characteristics, so that greater knowledge can be acquired which will guide the consideration of their potential application scenarios. With this in mind, a variety of spectroscopic and microscopic approaches by which such research into SBN' catalytic characteristics may be conducted have been subjected to concise consideration. An area of particular focus in this review is achieving environmentally friendly reactions in SBN. The researchers engaged in this project have been successful in establishing that SBN catalysts are applicable in a number of scenarios, and that they operate efficiently in, for example, producing benzyl acetate and adipic acid through the acetoxylation and oxidation of toluene and cyclohexane, respectively. In these respects, it has become evident that the presence of the second metal showed a very high significance in achieving a successful outcome.

It is worthy of note that recent times have seen significant developments in the control of bi-metal particle morphology, dimensions and synthetic techniques. Previous research has established that synthetic techniques and changes in chemical and redox situations can facilitate control of the bimetallic nanoparticles' form and morphology. The use of oxide carriers in the synthesis of stable bimetallic nanoparticles offers opportunities for different green applications that result from the unsupported metal nanoparticles unique characteristics with respect to combined or isolated atoms. SBN exhibits successful interactions that result in surface stabilization and the production of Lewis sites that may facilitate the catalyzing of particular reactions. The extent to which interactivity is achieved is dependent upon the nature of the support. SBN, therefore, offer the potential for varied and green use in a number of ways. It is clear that highly unsaturated systems generally offer a comparatively larger number of active surface metal regions that possibly offer interactivity between support and active phases that is more efficient and, consequently, are superior when compared to the alternatives. Stabilization and control of all bimetallic nanoparticles would represent a considerable advance that would facilitate the use of current homogenous catalysis methods and reactions to be used heterogeneously; however, commercial application is constrained by activity and selectivity characteristics. The stability and durability properties of SBN have interesting consequences in respect of productivity. The research reported in this thesis was largely motivated by the need to explore the function of SBN in a number of reactions performed in the liquid or gas phase, in addition to the need to explore their consequent catalytic processes. Research yet to be carried out may explore the production of bi-functional or multifunctional SBN that could have implications in respect of existing reactions, and could result in new products. It is clear that new techniques need to be developed that will enable the sequencing of various functionalities geared towards the development of new, attractive and environmentally friendly nanostructured metal nanoparticles for diverse catalytic applications.

Acknowledgments: The authors gratefully thank King Abdulaziz City for Science and Technology (KACST) and Leibniz institute for Catalysis (LIKAT) for financing this work. The authors also thank A. Benhmid for his discussions on improvements to this contribution.

Author Contributions: A.M. and V.N.K. designed the experiments. A.A. performed the materials synthesis, charactrization and test with the assistance of A.M. and V.N.K. Results analysis and manuscript preparation were done by A.A. and V.N.K and A.M. and A.A. supervised the project. All authors contributed to discussions and revision of the manuscript.

Conflicts of Interest: The author declares no conflict of interest.

References

1. Alexeev, O.S.; Gates, B.C. Supported Bimetallic Cluster Catalysts. *Ind. Eng. Chem. Res.* **2003**, *42*, 1571–1587. [CrossRef]
2. Campbell, C.T. Bimetallic Surface Chemistry. *Annu. Rev. Phys. Chem.* **1990**, *41*, 775–837. [CrossRef]
3. Sinfelt, J.H. *Bimetallic Catalysts: Discoveries, Concepts*; Wiley-Interscience: Hoboken, NJ, USA, 1983.
4. Somorjai, G.A.; Li, Y. *Introduction to Surface Chemistry and Catalysis*; John Wiley & Sons: Hoboken, NJ, USA, 2010.
5. Tao, F.F. Synthesis, catalysis, surface chemistry and structure of bimetallic nanocatalysts. *Chem. Soc. Rev.* **2012**, *41*, 7977–7979. [CrossRef] [PubMed]
6. Li, Y.; Somorjai, G.A. Nanoscale advances in catalysis and energy applications. *Nano Lett.* **2010**, *10*, 2289–2295. [CrossRef] [PubMed]
7. Bolz, F. *Advanced Materials in Catalysis*; Elsevier: London, UK, 2013.
8. Alonso, D.M.; Wettstein, S.G.; Dumesic, J.A. Bimetallic catalysts for upgrading of biomass to fuels and chemicals. *Chem. Soc. Rev.* **2012**, *41*, 8075–8098. [CrossRef] [PubMed]
9. Huynh, T.M.; Armbruster, U.; Pohl, M.-M.; Schneider, M.; Radnik, J.; Hoang, D.L.; Phan, B.M.Q.; Nguyen, D.A.; Martin, A. Hydrodeoxygenation of phenol as a model compound for bio-oil over non-noble bimetallic catalysts based on Ni. *ChemCatChem* **2014**, *6*, 1940–1951. [CrossRef]
10. Sankar, M.; Dimitratos, N.; Miedziak, P.J.; Wells, P.P.; Kiely, C.J.; Hutchings, G.J. Designing bimetallic catalysts for a green and sustainable future. *Chem. Soc. Rev.* **2012**, *41*, 8099–8139. [CrossRef] [PubMed]
11. Wei, Z.; Sun, J.; Li, Y.; Datye, A.K.; Wang, Y. Bimetallic catalysts for hydrogen generation. *Chem. Soc. Rev.* **2012**, *41*, 7994–8008. [CrossRef] [PubMed]
12. Jiang, T.; Zhou, Y.; Liang, S.; Liu, H.; Han, B. Hydrogenolysis of glycerol catalyzed by Ru-Cu bimetallic catalysts supported on clay with the aid of ionic liquids. *Green Chem.* **2009**, *11*, 1000–1006. [CrossRef]
13. Wettstein, S.G.; Bond, J.Q.; Alonso, D.M.; Pham, H.N.; Datye, A.K.; Dumesic, J.A. RuSn bimetallic catalysts for selective hydrogenation of levulinic acid to γ-valerolactone. *Appl. Catal. B* **2012**, *117*, 321–329. [CrossRef]
14. Ponec, V. On the role of promoters in hydrogenations on metals; α, β-unsaturated aldehydes and ketones. *Appl. Catal. A* **1997**, *149*, 27–48. [CrossRef]
15. Mäki-Arvela, P.; Hajek, J.; Salmi, T.; Murzin, D.Y. Chemoselective hydrogenation of carbonyl compounds over heterogeneous catalysts. *Appl. Catal. A* **2005**, *292*, 1–49. [CrossRef]
16. Lisowski, P.; Colmenares, J.C.; Lomot, D.; Chernyayeva, O.; Lisovytskiy, D. Preparation by sonophotodeposition method of bimetallic photocatalysts Pd-Cu/TiO2 for sustainable gaseous selective oxidation of methanol to methyl formate. *J. Mol. Catal. A Chem.* **2016**, *411*, 247–256. [CrossRef]
17. Sobczak, I.; Dembowiak, E. The effect of AuAg-MCF and AuAg-NbMCF catalysts pretreatment on the gold-silver alloy formation and the catalytic behavior in selective methanol oxidation with oxygen. *J. Mol. Catal. A Chem.* **2015**, *409*, 137–148. [CrossRef]
18. Mo, X.; Hu, H.; Tan, D.; Guo, T. Bimetallic gold-palladium supported on 5A zeolite and their catalytic activity for vinyl acetate synthesis. *Appl. Mech. Mate.* **2014**, 513–517. [CrossRef]
19. Zaleska-Medynska, A.; Marchelek, M.; Diak, M.; Grabowska, E. Noble metal-based bimetallic nanoparticles: The effect of the structure on the optical, catalytic and photocatalytic properties. *Adv. Colloid Interface Sci.* **2016**, *229*, 80–107. [CrossRef] [PubMed]
20. Cui, C.-H.; Li, H.-H.; Yu, S.-H. Large scale restructuring of porous Pt-Ni nanoparticle tubes for methanol oxidation: A highly reactive, stable, and restorable fuel cell catalyst. *Chem. Sci.* **2011**, *2*, 1611–1614. [CrossRef]
21. Bin Saiman, M.I.; Brett, G.L.; Tiruvalam, R.; Forde, M.M.; Sharples, K.; Thetford, A. Involvement of Surface-Bound Radicals in the Oxidation of Toluene Using Supported Au-Pd Nanoparticles. *Angew. Chem. Int. Ed.* **2012**, *51*, 5981–5986. [CrossRef] [PubMed]

22. Jirkovský, J.S.; Panas, I.; Ahlberg, E.; Halasa, M.; Romani, S.; Schiffrin, D.J. Single atom hot-spots at Au-Pd nanoalloys for electrocatalytic H_2O_2 Production. *J. Am. Chem. Soc.* **2011**, *133*, 19432–19441. [CrossRef] [PubMed]
23. Mohl, M.; Dobo, D.; Kukovecz, A.; Konya, Z.; Kordas, K.; Wei, J. Formation of CuPd and CuPt bimetallic nanotubes by galvanic replacement reaction. *J. Phys. Chem. C.* **2011**, *115*, 9403–9409. [CrossRef]
24. Huang, Q.; Yang, H.; Tang, Y.; Lu, T.; Akins, D.L. Carbon-supported Pt-Co alloy nanoparticles for oxygen reduction reaction. *Electrochem. Commun.* **2006**, *8*, 1220–1224. [CrossRef]
25. Mohamed, M.B.; Volkov, V.; Link, S.; El-Sayed, M.A. The 'lightning' gold nanorods: Fluorescence enhancement of over a million compared to the gold metal. *Chem. Phys. Lett.* **2000**, *317*, 517–523. [CrossRef]
26. Lee, K.-S.; El-Sayed, M.A. Gold and silver nanoparticles in sensing and imaging: Sensitivity of plasmon response to size, shape, and metal composition. *J. Phys. Chem. Lett. B* **2006**, *110*, 19220–19225. [CrossRef] [PubMed]
27. Cheng, M.-T.; Liu, S.-D.; Wang, Q.-Q. Modulating emission polarization of semiconductor quantum dots through surface plasmon of metal nanorod. *Appl. Phys. Lett.* **2008**, *92*, 162107–162110. [CrossRef]
28. Wang, H.; Brandl, D.W.; Le, F.; Nordlander, P.; Halas, N.J. Nanorice: A hybrid plasmonic nanostructure. *Nano Lett.* **2006**, *6*, 827–832. [CrossRef] [PubMed]
29. Kreibig, U.; Vollmer, M. *Optical Properties of Metal Clusters*; Springer Science & Business Media: Berlin, Germany, 2013.
30. Kim, K.; Kim, K.L.; Choi, J.-Y.; Lee, H.B.; Shin, K.S. Surface enrichment of Ag atoms in Au/Ag Alloy nanoparticles revealed by surface-enhanced Raman scattering of 2, 6-dimethylphenyl isocyanide. *J. Phys. Chem. C* **2010**, *114*, 3448–3453. [CrossRef]
31. Ramakritinan, C.M.; Kaarunya, E.; Shankar, S.; Kumaraguru, A.K. Antibacterial effects of Ag, Au and bimetallic (Ag-Au) nanoparticles synthesized from red algae. *Solid State Phenom.* **2013**, *201*, 211–230. [CrossRef]
32. Liu, X.; Wang, D.; Li, Y. Synthesis and catalytic properties of bimetallic nanomaterials with various architectures. *Nano Today* **2012**, *7*, 448–466. [CrossRef]
33. Kyriakou, G.; Boucher, M.B.; Jewell, A.D.; Lewis, E.A.; Lawton, T.J.; Baber, A.E. Isolated metal atom geometries as a strategy for selective heterogeneous hydrogenations. *Science* **2012**, *335*, 1209–1212. [CrossRef] [PubMed]
34. Zhang, H.; Watanabe, T.; Okumura, M.; Haruta, M.; Toshima, N. Catalytically highly active top gold atom on palladium nanocluster. *Nat. Mater.* **2012**, *11*, 49–52. [CrossRef] [PubMed]
35. Cheng, K.; Sun, S. Recent advances in syntheses and therapeutic applications of multifunctional porous hollow nanoparticles. *Nano Today* **2010**, *5*, 183–196. [CrossRef]
36. An, K.; Hyeon, T. Synthesis and biomedical applications of hollow nanostructures. *Nano Today* **2009**, *4*, 359–373. [CrossRef]
37. Zhang, Q.; Wang, W.; Goebl, J.; Yin, Y. Self-templated synthesis of hollow nanostructures. *Nano Today* **2009**, *4*, 494–507. [CrossRef]
38. Lim, B.; Jiang, M.; Yu, T.; Camargo, P.H.; Xia, Y. Nucleation and growth mechanisms for Pd-Pt bimetallic nanodendrites and their electrocatalytic properties. *Nano Res.* **2010**, *3*, 69–80. [CrossRef]
39. Krylova, G.; Giovanetti, L.J.; Requejo, F.G.; Dimitrijevic, N.M.; Prakapenka, A.; Shevchenko, E.V. Study of nucleation and growth mechanism of the metallic nanodumbbells. *J. Am. Chem. Soc.* **2012**, *134*, 4384–4392. [CrossRef] [PubMed]
40. Jiang, H.-L.; Akita, T.; Ishida, T.; Haruta, M.; Xu, Q. Synergistic catalysis of Au@Ag core-Shell nanoparticles stabilized on metal-organic framework. *J. Am. Chem. Soc.* **2011**, *133*, 1304–1306. [CrossRef] [PubMed]
41. Huang, X.; Tang, S.; Liu, B.; Ren, B.; Zheng, N. Enhancing the Photothermal Stability of Plasmonic Metal Nanoplates by a Core-Shell Architecture. *Adv. Mater.* **2011**, *23*, 3420–3425. [CrossRef] [PubMed]
42. Yoo, W.-J.; Miyamura, H.; Kobayashi, S. Polymer-Incarcerated Gold-Palladium Nanoclusters with Boron on Carbon: A Mild and Efficient Catalyst for the Sequential Aerobic Oxidation-Michael Addition of 1, 3-Dicarbonyl Compounds to Allylic Alcohols. *J. Am. Chem. Soc.* **2011**, *133*, 3095–3103. [CrossRef] [PubMed]
43. Singh, S.K.; Singh, A.K.; Aranishi, K.; Xu, Q. Noble-metal-free bimetallic nanoparticle-catalyzed selective hydrogen generation from hydrous hydrazine for chemical hydrogen storage. *J. Am. Chem. Soc.* **2011**, *133*, 19638–19641. [CrossRef] [PubMed]
44. Suryanarayana, C. Mechanical alloying and milling. *Prog. Mater. Sci.* **2001**, *46*, 1–184. [CrossRef]

45. Haruta, M.; Daté, M. Advances in the catalysis of Au nanoparticles. *Appl. Catal. A* **2001**, *222*, 427–437. [CrossRef]
46. Pileni, M. Nanosized particles made in colloidal assemblies. *Langmuir* **1997**, *13*, 3266–3276. [CrossRef]
47. Fu, X.; Wang, Y.; Wu, N.; Gui, L.; Tang, Y. Shape-selective preparation and properties of oxalate-stabilized Pt colloid. *Langmuir* **2002**, *18*, 4619–4624. [CrossRef]
48. Toshima, N.; Kuriyama, M.; Yamada, Y.; Hirai, H. Colloidal platinum catalyst for light-induced hydrogen evolution from water. A particle size effect. *Chem. Lett.* **1981**, *10*, 793–806. [CrossRef]
49. Lopez, N.; Janssens, T.; Clausen, B.; Xu, Y.; Mavrikakis, M.; Bligaard, T. On the origin of the catalytic activity of gold nanoparticles for low-temperature CO oxidation. *J. Catal.* **2004**, *223*, 232–235. [CrossRef]
50. Friebel, D.; Miller, D.J.; Nordlund, D.; Ogasawara, H.; Nilsson, A. Degradation of Bimetallic Model Electrocatalysts: An In Situ X-Ray Absorption Spectroscopy Study. *Angew. Chem. Int. Ed.* **2011**, *50*, 10190–10192. [CrossRef] [PubMed]
51. Ono, L.; Sudfeld, D.; Cuenya, B.R. In situ gas-phase catalytic properties of TiC-supported size-selected gold nanoparticles synthesized by diblock copolymer encapsulation. *Surf. Sci.* **2006**, *600*, 5041–5050. [CrossRef]
52. Cuenya, B.R. Synthesis and catalytic properties of metal nanoparticles: Size, shape, support, composition, and oxidation state effects. *Thin Solid Films* **2010**, *518*, 3127–3150. [CrossRef]
53. Molenbroek, A.M.; Nørskov, J.K.; Clausen, B.S. Structure and reactivity of Ni-Au nanoparticle catalysts. *J. Phys. Chem. B* **2001**, *105*, 5450–5458. [CrossRef]
54. Besenbacher, F.; Chorkendorff, I.I.; Clausen, B.S.; Hammer, B.; Molenbroek, A.M.; Nørskov, J.K.; Stensgaard, I.I. Design of a surface alloy catalyst for steam reforming. *Science* **1998**, *279*, 1913–1918. [CrossRef] [PubMed]
55. Meille, V. Review on methods to deposit catalysts on structured surfaces. *Appl. Catal. A* **2006**, *315*, 1–17. [CrossRef]
56. Chen, M.; Goodman, D. The structure of catalytically active gold on titania. *Science* **2004**, *306*, 252–257. [CrossRef] [PubMed]
57. Prati, L.; Villa, A. The art of manufacturing gold catalysts. *Catalysts* **2011**, *2*, 24–37. [CrossRef]
58. Nishimura, S.; Takagaki, A.; Ebitani, K. Characterization, synthesis and catalysis of hydrotalcite-related materials for highly efficient materials transformations. *Green Chem.* **2013**, *15*, 2026–2042. [CrossRef]
59. Debecker, D.P.; Mutin, P.H. Non-hydrolytic sol-gel routes to heterogeneous catalysts. *Chem. Soc. Rev.* **2012**, *41*, 3624–3650. [CrossRef] [PubMed]
60. Ciriminna, R.; Fidalgo, A.; Pandarus, V.; Béland, F.; Ilharco, L.M.; Pagliaro, M. The sol-gel route to advanced silica-based materials and recent applications. *Chem. Rev.* **2013**, *113*, 6592–6620. [CrossRef] [PubMed]
61. Esparza, R.; Téllez-Vázquez, O.; Ángeles-Pascual, A.; Pérez, R. Synthesis and characterization of bimetallic nanoparticles by cs-corrected scanning transmission electron microscopy. In *Materials Characterization*; Springer: Basel, Switzerland, 2015; pp. 35–42.
62. Fedlheim, D.L.; Foss, C.A. *Metal Nanoparticles: Synthesis, Characterization, and Applications*; CRC Press: New York, NY, USA, 2001.
63. Gontard, L.C.; Chang, L.Y.; Hetherington, C.J.; Kirkland, A.I.; Ozkaya, D.; Dunin-Borkowski, R.E. Aberration-Corrected Imaging of Active Sites on Industrial Catalyst Nanoparticles. *Angew. Chem. Int. Ed.* **2007**, *119*, 3757–3759. [CrossRef]
64. Zhou, W.; Wachs, I.E.; Kiely, C.J. Nanostructural and chemical characterization of supported metal oxide catalysts by aberration corrected analytical electron microscopy. *Curr. Opin. Solid State Mater. Sci.* **2012**, *16*, 10–22. [CrossRef]
65. Akita, T.; Kohyama, M.; Haruta, M. Electron microscopy study of gold nanoparticles deposited on transition metal oxides. *Acc. Chem. Res.* **2013**, *46*, 1773–1782. [CrossRef] [PubMed]
66. Tozzola, G.; Mantegazza, M.; Ranghino, G.; Petrini, G.; Bordiga, S.; Ricchiardi, G. On the structure of the active site of Ti-silicalite in reactions with hydrogen peroxide: A vibrational and computational study. *J. Catal.* **1998**, *179*, 64–71. [CrossRef]
67. Lee, H.; Habas, S.E.; Kweskin, S.; Butcher, D.; Somorjai, G.A.; Yang, P. Morphological control of catalytically active platinum nanocrystals. *Angew. Chem. Int. Ed.* **2006**, *118*, 7988–7992. [CrossRef]
68. Zhang, W.; Luo, X.-J.; Niu, L.-N.; Yang, H.-Y.; Yiu, C.K.; Zhou, L.-Q. Biomimetic Intrafibrillar Mineralization of Type I Collagen with Intermediate Precursors-loaded Mesoporous Carriers. *Sci. Rep.* **2015**, *5*, 11199–11210. [CrossRef] [PubMed]

69. Jackson, S.D.; Hargreaves, J.S. *Metal oxide catalysis*; Wiley Online Library: Berlin, Germany, 2009.
70. Schoonheydt, R.A. UV-VIS-NIR spectroscopy and microscopy of heterogeneous catalysts. *Chem. Soc. Rev.* **2010**, *39*, 5051–5066. [CrossRef] [PubMed]
71. Che, M.; Védrine, J.C. *Characterization of Solid Materials and Heterogeneous Catalysts: From structure to surface reactivity*; John Wiley & Sons: Hoboken, NJ, USA, 2012. [CrossRef]
72. Busca, G. The Use of Infrared Spectroscopic Methods in the Field of Heterogeneous Catalysis by Metal Oxides. In *Metal Oxide Catalysis*; WILEY-VCH Verlag GmbH & Co. KGaA: Weinheim, Germany, 2009; pp. 95–175. [CrossRef]
73. Pan, X.; Fan, Z.; Chen, W.; Ding, Y.; Luo, H.; Bao, X. Enhanced ethanol production inside carbon-nanotube reactors containing catalytic particles. *Nat. Mater.* **2007**, *6*, 507–511. [CrossRef] [PubMed]
74. Borodko, Y.; Habas, S.E.; Koebel, M.; Yang, P.; Frei, H.; Somorjai, G.A. Probing the interaction of poly (vinylpyrrolidone) with platinum nanocrystals by UV-Raman and FTIR. *J. Phys. Chem. B* **2006**, *110*, 23052–23059. [CrossRef] [PubMed]
75. Rivière, J.C.; Myhra, S. *Handbook of Surface and Interface Analysis: Methods for Problem-Solving*; CRC Press: Boca Raton, FL, USA, 2009. [CrossRef]
76. Benhmid, A.; Narayana, K.V.; Martin, A.; Lücke, B.; Pohl, M.-M. Highly Active and Selective Pd-Cu-TiO_2 catalyst for the direct synthesis of benzyl acetate by gas phase acetoxylation of toluene. *Chem. Lett.* **2004**, *33*, 1238–1239. [CrossRef]
77. Radnik, J.; Benhmid, A.; Kalevaru, V.N.; Pohl, M.M.; Martin, A.; Lücke, B.; Dingerdissen, U. Deactivation of Pd acetoxylation catalysts: Direct observations by XPS investigations. *Angew. Chem. Int. Ed.* **2005**, *44*, 6771–6774. [CrossRef] [PubMed]
78. Radnik, J.; Pohl, M.-M.; Kalevaru, V.N.; Martin, A. First knowledge on the formation of novel core-shell structures in PdCu catalysts and their influence on the prevention of catalyst deactivation. *J. Phys. Chem. C* **2007**, *111*, 10166–10169. [CrossRef]
79. Benhmid, A.; Narayana, K.V.; Martin, A.; Lücke, B.; Bischoff, S.; Pohl, M.-M.; Radnik, J.; Schneider, M. Highly efficient Pd-Sb-TiO_2 catalysts for the vapour phase acetoxylation of toluene to benzyl acetate. *J. Catal.* **2005**, *230*, 420–435. [CrossRef]
80. Benhmid, A.; Narayana, K.V.; Radnik, J.; Martin, A.; Lücke, B. Effect of Sb loading on Pd nanoparticles and its influence on the catalytic performance of Sb-Pd/TiO2 solids for acetoxylation of toluene. *J. Catal.* **2006**, *243*, 25–35. [CrossRef]
81. Gatla, S.; Radnik, J.; Madaan, N.; Pohl, M.-M.; Mathon, O.; Rogalev, A.; Kalevaru, V.N.; Martin, A.; Pascarelli, S.; Brueckner, A. New insights into the nature of co-components and their impact on Pd-structure: X-ray absorption studies on toluene acetoxylation studies. *Chem. Eur. J.* **2015**, *21*, 15280–15289. [CrossRef] [PubMed]
82. Shu, Q.; Wang, X.; Ren, S.; Shi, W. Gas-phase oxidative acetoxylation of toluene over Pd-Sn-K/SiO_2 catalyst. *Cuihua Xuebao* **2005**, *26*, 869–873.
83. Komatsu, T.; Inaba, K.; Uezono, T.; Onda, A.; Yashima, T. Nano-size particles of palladium intermetallic compounds as catalysts for oxidative acetoxylation. *Appl. Catal. A* **2003**, *251*, 315–326. [CrossRef]
84. Alshammari, A.; Koeckritz, A.; Kalevaru, V.N.; Bagabas, A.; Martin, A. Potential of Supported Gold Bimetallic Catalysts for Green Synthesis of Adipic Acid from Cyclohexane. *Top. Catal.* **2015**, *58*, 1069–1076. [CrossRef]
85. Alshammari, A.; Koeckritz, A.; Kalevaru, V.N.; Bagabas, A.; Martin, A. Significant Formation of Adipic Acid by Direct Oxidation of Cyclohexane Using Supported Nano-Gold Catalysts. *Chem. Cat. Chem.* **2012**, *4*, 1330–1336. [CrossRef]
86. Hereijgers, B.P.C.; Weckhuysen, B.M. Aerobic oxidation of cyclohexane by gold-based catalysts: New mechanistic insight by thorough product analysis. *J. Catal.* **2010**, *270*. [CrossRef]